IGNITION TARGET DESIGN FOR THE NATIONAL IGNITION FACILITY

S. W. Haan	*P. A. Amendt*	*G. L. Strobel*	*D. B. Harris**
S. M. Pollaine	*J. A. Futterman*	*M. Tabak*	*N. M. Hoffman**
J. D. Lindl	*W. K. Levedahl*	*S. V. Weber*	*B. H. Wilde**
L. J. Suter	*M. D. Rosen*	*G. B. Zimmerman*	*W. S. Varnum**
R. L. Berger	*D. P. Rowley*	*W. J. Krauser**	*F. J. Swenson**
L. V. Powers	*R. A. Sacks*	*D. C. Wilson**	*P. A. Bradley**
W. E. Alley	*A. I. Shestakov*	*S. Coggeshall**	

Introduction

The goal[1,2] of inertial confinement fusion (ICF) is to produce significant thermonuclear burn from a target driven with a laser or ion beam. To achieve that goal, the national ICF Program has proposed a laser capable of producing ignition and intermediate gain.[3] The facility is called the National Ignition Facility (NIF). This article describes ignition targets designed for the NIF[4] and their modeling. Although the baseline NIF target design, described herein, is indirect drive, the facility will also be capable of doing direct-drive ignition targets—currently being developed at the University of Rochester.[5]

Figure 1 illustrates the baseline target, which is typical of all our ignition targets. A spherical cryogenic capsule, composed of deuterium–tritium (DT) gas, DT solid fuel, and an ablator, is encased in a cylindrical Au hohlraum with two laser entrance holes (LEHs) at opposite ends. The hohlraum peak radiation temperature (T_R) is 250–300 eV, with a shaped prepulse for a low-entropy implosion. The ablation pressure allows the fuel shell to reach a velocity of $3–4 \times 10^7$ cm/s. The central part of the DT is then compressed and heated, forming a hot spot that reaches ignition conditions of density times radius $\rho r \sim 0.3$ g/cm^2 and ion temperature ~10 keV. Then, α deposition "bootstraps" the central temperature to >30 keV. The hot-spot density at ignition is typically 75–100 g/cm^3. The hot spot is tamped by a colder main fuel layer, with $\rho\Delta r \approx 1$ g/cm^2 and density ≈1000 g/cm^3. The burn propagates into the main fuel layer, and 10–15% of the total DT mass is

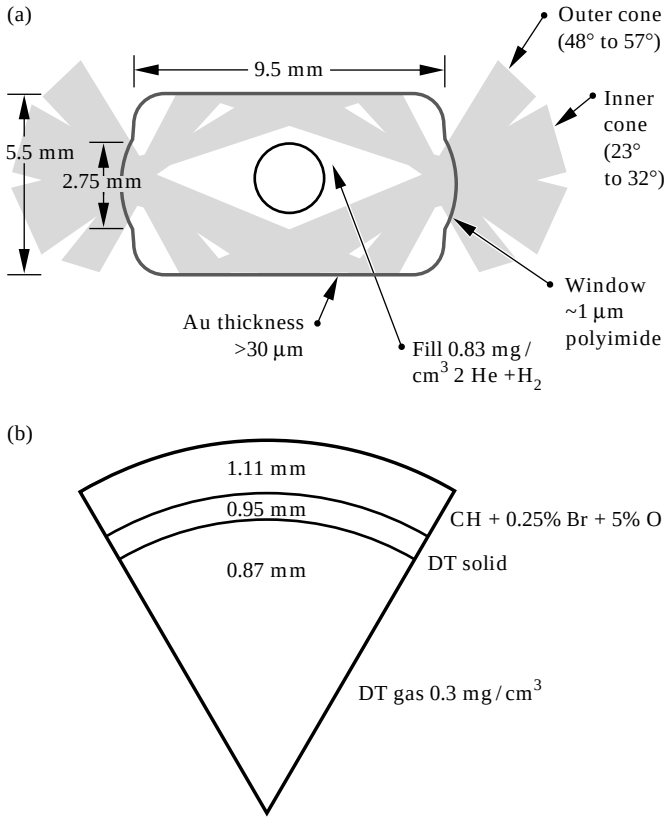

FIGURE 1. This ignition target (referred to as the point-design target or PT) uses 1.35 MJ of laser energy. (a) Shows the entire target, and (b) shows details of the central spherical capsule. The DT fuel is in a cryogenic layer, surrounded by a CH ablator doped with 0.25% Br. The capsule is in the center of a Au hohlraum, which the incoming laser beams heat to 300 eV. The beams are arranged in two cones entering from opposite sides. (50-05-0494-1802pb01)

*Los Alamos National Laboratory, Los Alamos, New Mexico

burned. The target shown in Fig. 1 produces 10–15 MJ of yield in simulations, depending on the modeling used.

Assuming the laser meets other specifications, the two most important laser parameters determining the margin for ignition are the total energy and the peak power.[6] Ignition requires both energy and power, as indicated in Fig. 2. The ignition region is bounded on one side by hydrodynamic instabilities. Ultimately, this boundary of the ignition region is determined by the capsule surface smoothness; Fig. 2 assumes the surface finish currently achieved on Nova capsules in modeling described in this article. On the other side, the ignition region is bounded by laser–plasma instabilities. Laser intensity and other parameters determining the instabilities (especially the electron density n_e) depend primarily on the desired peak hohlraum T_R. Estimates of the laser–plasma instabilities, described here, indicate that laser–plasma instabilities will be acceptable in targets driven to at least 320 eV (shown as the upper boundary of the ignition region in Fig. 2).

The smallest possible ignition target with this assumed surface finish, at 0.8 MJ and 300 TW, would have no remaining margin for uncertainties or errors in the target modeling. We have specified the NIF at 1.8 MJ and 500 TW to provide margin for such uncertainties. This margin is adequate to cover our estimates of energetically significant uncertainties, as described in this article.

Baseline Ignition Targets

Figure 1 shows the baseline design, referred to as the PT: "point-design target." Cryogenic hardware, not shown, is external to the hohlraum. The spherical capsule is a doped CH ablator around a shell of solid cryogenic DT. The solid DT layer is self-smoothing, because of the β-smoothing effect.[7] The cryogenic temperature controls the density of the central DT gas. The hohlraum is filled with a 50–50 (atomic) mixture of He and H. This gas conducts away the β decay energy before the target is shot and maintains the open hohlraum cavity during the implosion. The mixture of gases minimizes stimulated Brillouin scattering (SBS).

The PT uses 1.35 MJ of 3ω light, which is intermediate between the full 1.8 MJ and the "ignition cliff" at 800 kJ. Most of our modeling concentrates on this intermediate-scale target. It is sufficiently robust that we can make a good case for its ignition, while it leaves margin for uncertainty with a 1.8-MJ facility. Also, by using a relatively small target to set specifications for power balance, pointing, target fabrication quality, and so forth, we can be sure that the specifications are adequate for a range of likely targets.

Figure 3 shows an optimal T_R profile for the capsule, used as input to our capsule modeling, and an input laser profile. The target can tolerate moderate deviations from the nominal profile. For example, Fig. 4 shows the yield from integrated calculations (described later in more detail) as the duration of the peak power portion of the pulse is varied. Our robustness study of the PT is described in more detail below.

The light entering each LEH is in two cones, as shown in Fig. 1, and we can minimize time-dependent asymmetry in the x radiation incident on the capsule by dynamically varying the relative power of the cones. About one third of the energy must go into the waist

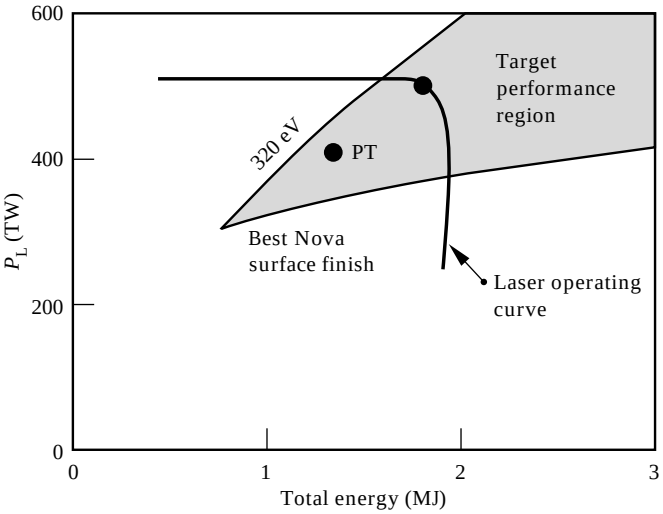

FIGURE 2. Total laser energy and peak power determine the margin for ignition. Powers and energies along the indicated curve will be accessible to the NIF, as currently planned. The upper dot illustrates the laser's nominal operating point (1.8 MJ, 500 TW); the lower dot illustrates the energy and power needed to drive the PT (1.35 MJ, 410 TW). (50-05-0494-1805pb01)

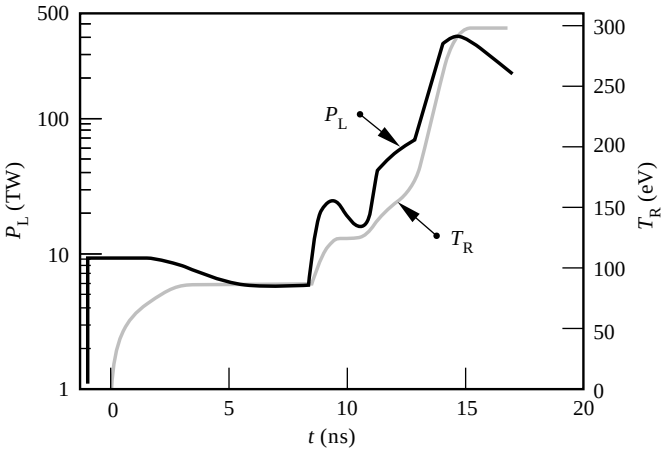

FIGURE 3. Temperature vs time optimal for the PT capsule, and laser power vs time to drive the target. The shaped pulse prior to peak drive is needed to compress the target, increasing the pressure in a controlled way before applying peak power. The gray curve is the radiation temperature vs time that drives capsule simulations, and the black curve is the laser power vs time used as input to hohlraum simulations. (50-05-0295-0395pb01)

cones. The 192 beams are clustered in groups of four, so that there are effectively 48 spots. These are divided as 8 spots in each of the inner cones and 16 in the outer cones. We may use slightly separate wavelengths in the four beams in each spot to limit laser–plasma instabilities. The four beams combine at an angle corresponding to an effective $f/8$ optic.

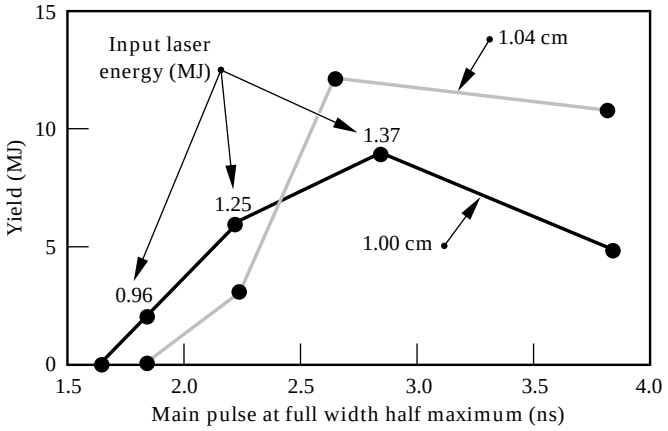

FIGURE 4. Yield vs duration of the peak power pulse, from integrated 2-D simulations. The pulse width changes by varying the cut-off time. The energy in a sample of the pulses is shown. The failure at short pulse appears to be due to asymmetry, not energetic failure to ignite. Two different hohlraum lengths, providing different symmetry "tunes," are shown. (50-05-0295-0388pb01)

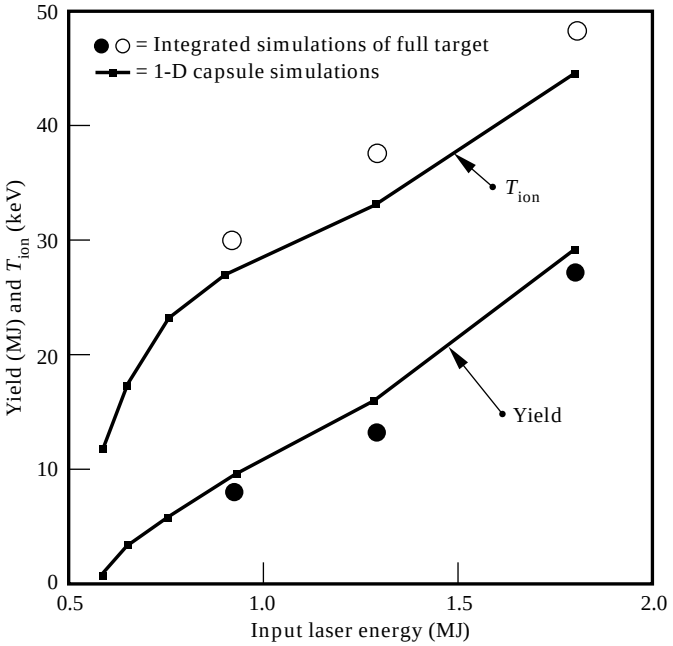

FIGURE 5. Yield and burn-weighted ion temperature for geometric scales of the PT. The lines show 1-D calculations of the capsule alone, in which linear dimensions and times are scaled together (the horizontal scale is effective energy, that is, 1.35 MJ times the scale factor cubed; the dots are integrated calculations, plotted against the laser energy). For these, linear dimensions and times were scaled, and laser powers were scaled as the square of the scale factor. Hohlraum length and cone-to-cone power ratios were adjusted to recover symmetry. (50-05-0295-0389pb01)

Each beam is focused to an elliptical spot, with the minor axis in the plane of the laser ray and the hohlraum axis. This maximizes the LEH clearance while minimizing the laser intensity. The spot has a shape approximating a flat top (probably a sixth-order super-Gaussian), again to minimize the peak intensity while maximizing LEH clearance. The nominal spot is 500 μm × 1000 μm at best focus. Such a spot can be made with recently developed kinoform phase plate techniques.[8]

The pulse shape shown in Fig. 3 creates four shocks, with the final shock bringing the ablator up to peak pressure with sufficiently low DT entropy. The entropy requirement implies a corresponding requirement on the precision of the pulse shaping. For optimal performance, the shocks must be timed within about 200 ps. Adequate shock timing may not be predictable *a priori* given uncertainties in opacity and equation-of-state (EOS), but is achievable with an experimental program using techniques currently in use on Nova.[9]

The CH ablator contains 0.25% Br dopant. (Some Nova targets currently use Br-doped CH.[10]) The dopant is used to control the stability of the ablator / DT interface. It reduces the preheat in the CH and eliminates an unstable density step at the CH / DT interface. The CH is assumed to contain 5% O as an incidental fabrication by-product.

We conclude this section with a brief description of our baseline one-dimensional (1-D) capsule simulations. These simulations are performed with the LASNEX code,[11] using Legendre decomposed radiation transport,[12] EOSs calculated in line with a "Quotidian EOS" package,[13] and average-atom opacities calculated with the XSN code.[14] We have also simulated the capsule implosion with other radiation transport schemes, but find no difference in the calculations. Implosion calculations use as a source nonPlanckian frequency-dependent radiation determined from hohlraum simulations. The spectrum affects the short-wavelength hydrodynamic instability growth; other than this, the spectrum has little effect on target characteristics. We normally calculate the deposition of α particles produced by the burn with the multigroup diffusion package in LASNEX.[15] Hatchett[16] performed a baseline 1-D simulation of the PT using a Monte Carlo charged-particle transport code[17] and found that the ignition and burn are essentially the same as with multigroup charged-particle diffusion.

Other Possible Ignition Targets

Modeling of a wide variety of other targets has been performed at various levels of detail. Several important aspects of the target can be varied, providing

different trade-offs of the remaining uncertainties in our understanding.

We can vary the size of the target, and the energy it uses. Direct geometric scales of the PT produce good burn at any laser energy above about 700 kJ, as shown in Fig. 5. This energy margin allows for loss of energy to stimulated scattering processes and laser coupling. Also, it allows us, if necessary, to change the relative size of the hohlraum and capsule. This allows a trade-off of the capsule ignition physics, and hydrodynamic instability, with symmetry and hohlraum filling.

The knee at 600–800 kJ in Fig. 5 and the two thresholds at 1.6 and 1.8 ns in Fig. 4 are typical signatures of ignition. Without α deposition and thermonuclear bootstrapping, NIF targets would be expected to produce no more than 10–100 kJ of yield at the likely ion temperatures of less than about 10 keV. Experimental demonstration of ignition will be clear when we do a series of targets that scan through the threshold between such a non-bootstrapping mode and burn producing about 1 MJ or more. This could be done by varying the target size, as shown in Fig. 5, or more likely by varying the implosion velocity (implicit in Fig. 4). Varying the D to T ratio will provide another easy-to-interpret lever on the burn rate. Curves of yield vs implosion velocity, for various D to T ratios, should show an inflection and a large increase in yield when the burn threshold is crossed for ratios near 50–50.

Various other target designs, described next, are at various scales in the ignition range.

Uncertainty in ablation characteristics can be addressed by using other ablator materials. In particular, Be generally performs better than CH as an ablator. (The PT uses a CH ablator because of fabrication experience with Nova.[18]) Be must be doped more heavily than CH, and radially varying the doping allows for complete optimization. Designs exist in which the Be is doped with Cu, which appears attractive from a fabrication point of view, and others with a mixture of Na and Br. In the most highly optimized targets, the additional performance margin obtained by using Be instead of CH is equivalent to about 25 eV in peak hohlraum T_R. The advantage is better at 250 eV than at 300 eV.

Another important advantage of Be is more hydrodynamic stability. Using the modeling described below in the section on hydrodynamic instabilities, we have found a clear advantage to Be targets. Because it ablates faster, Be is more stable—the initial mass of the Be ablator is nearly twice that of the CH. The outer surface roughness specification is somewhat looser for Be than for CH, but the most important difference is in the required surface quality for the inner surface of the DT ice. Perturbations initially on the ice grow by coupling to the outer surface, the unstable ablation front, during acceleration; this coupling is much less effective through the more massive Be shell. As a result, a Be target (driven at 300 eV) can tolerate about four times larger perturbations initially on the inner surface of the ice than a CH target.

We can modify the convergence ratio (defined as the initial outer radius of the ablator divided by the ignition-time hot-spot radius) by varying the initial central DT gas density. Since reducing the convergence ratio reduces the final ρr, it also reduces the yield. If the initial gas fill is increased the ignition is marginal, i.e., the yield is reduced from 15 MJ nominal to about 1 MJ. These low-convergence targets require gas densities that would initially be in vapor equilibrium with liquid DT (as opposed to solid for the PT), and fielding them will require some modifications in the fabrication and fielding technology. The triple-point gas density,[19] 0.68 mg/cm^3, corresponds to a PT yield of 10 MJ.

Various peak drive temperatures are possible—high temperatures stress laser–plasma instabilities while minimizing hydrodynamic instabilities, and low temperatures provide the opposite trade-off. The baseline is 300 eV, a compromise between the two constraints. We have designed capsules driven at temperatures as high as 400 eV that appear to be very resistant to hydrodynamic instabilities. Using doped Be as an ablator, we have designed targets driven at 250-eV for which ignition is nearly as robust as with CH at 300 eV. Laser–plasma instabilities are estimated to be very benign in the 250-eV hohlraum.

There is also a wide variety of possible pulse shapes. The pulse shown in Fig. 3 has four pulses or steps, each at a time and power to launch a shock, as needed, for the low-entropy implosion. Many other pulses can result in the same shocks in the fuel. We can use shorter pulses at higher powers (sometimes called "picket fence pulses"); we have used steps with the power held constant for a few nanoseconds in each step; at the other extreme, we have used pulses in which the power increases smoothly from an initial 10 TW up to peak power. Each of these shapes represents a different trade-off of laser, hohlraum, and capsule physics.

We have also designed targets in which the solid DT fuel is supported in a foam layer.[20] This may be an important option if β layering is inadequate. DT-wettable foams of density 0.05 g/cm^3 with micrometer-scale cell structure have been fabricated, and our designs assume this density. The foam targets work nearly as well as the solid DT targets. If β layering, or some other technique, can be used to maintain a pure DT layer about 10 μm thick on the inside of a foam-supported main fuel layer, ignition occurs in clean DT and target performance is barely degraded by the presence of the foam. If all of the solid DT must be supported by foam, it is somewhat more difficult to ignite, although targets at the PT scale still ignite with some remaining margin.

There are numerous possible ignition designs that have attractive features, and may actually perform better

than the point design, but that are not as closely connected to the existing experimental data. Direct-drive targets are an important option, pending experimental results from the Omega Upgrade at the University of Rochester. Other hohlraum designs are being investigated on Nova—for example, Au shields placed between the capsule and the LEHs can reduce the time-dependent asymmetry. Recent results on Nova for such a hohlraum are in excellent agreement with expectations based on simulations.[21] As the NIF is being planned and built, experiments on Nova will continue to refine our understanding of the target physics and will allow us to optimize the NIF design further.

So far we have described the various target options that work according to current modeling; we have also found two target concepts where our modeling predicts difficulties:

- We considered lining the hohlraum with CH, instead of the He / H gas fill described earlier. However, we find that the lining stagnates on axis, creating a pressure spike that perturbs the capsule implosion unacceptably. Unfilled hohlraums have too much Au absorption of the light. We intend to consider alternate liners and unfilled hohlraums with short, low-temperature pulses.
- In principle, it seems possible to achieve ignition with noncryogenic gaseous DT. However, we have found that the implosion velocities required for ignition at the NIF scale result in high core temperatures before ignition ρr is reached, and then conduction from the hot spot is very high. In a cryogenic target, energy conducted from the hot spot into the DT pusher heats more DT—this increases the mass of the hot spot, and the energy is not lost. If the hot spot is surrounded by inert material, the energy is not only lost from the fuel, but it serves to degrade the compressibility of the pusher. Rayleigh–Taylor (RT) instabilities would also be much more problematic if the igniting fuel were surrounded with inert material. Therefore, we have been unable to calculate ignition successfully in noncryogenic capsules at the NIF scale.

Hohlraum Design and Modeling

The size of the hohlraum relative to the capsule is determined by a variety of trade-offs. The required profile of T_R vs time is determined by the capsule, and any hohlraum larger than some minimum size could provide the needed T_R vs time profile. A larger hohlraum takes more laser energy and power, and the optimal size is a trade-off of the energy and power requirements and the need for symmetry and acceptable plasma filling. Our modeling indicates that the symmetry and laser–plasma instabilities are acceptable in the baseline hohlraum. Assuming a 1.8-MJ, 500-TW NIF, there will be margin to increase the hohlraum size with the PT capsule, increasing the margin for laser–plasma instabilities or asymmetry. If necessary, we can further increase this margin by using a smaller capsule, at the cost of either increasing hydrodynamic instabilities or developing Be-ablator fabrication technology.

Even with perfect laser pointing and beam-to-beam power balance, there is some asymmetry that we call the intrinsic asymmetry. This asymmetry arises because of the LEH and the bright laser-irradiated spots (the LEH alone causes a 15% peak-to-valley asymmetry). As described in Ref. 6, the laser spots are placed to cancel the LEH asymmetry. The symmetry can be adjusted by changing the hohlraum length and the pointing of the beams. The quantities determining the intrinsic symmetry change in time: the LEH shrinks, the laser spots move due to plasma evolution, and the spots become less bright relative to the overall hohlraum brightness. With a single cone of beams, we found that the time-dependent asymmetry was too large. Two cones of beams can be arranged to provide adequate symmetry. Also, with two cones the time-dependent asymmetry can be corrected dynamically by varying the relative power in the cones as a function of time. This detailed symmetry tuning will have to be done with a time-dependent symmetry campaign similar to those being done on the Nova laser.[22]

To model the intrinsic asymmetry, we use a detailed two-dimensional (2-D) simulation with a radiation-hydrodynamics code such as LASNEX.[13] We use the best available radiation transport model for the hohlraum / capsule coupling, and simulations are continued all the way through burn. The simulations track the laser beams, calculating inverse Bremsstrahlung energy deposition and any refraction that occurs. We typically use XSN nonLTE multigroup opacities,[16] although we have also performed simulations with an opacity table derived from the super transition array opacity model.[23] Any coupling to the capsule via hydrodynamic pressure or electron conduction is included.

We have achieved adequate symmetry and good burn in such integrated simulations of a variety of designs: the PT at several scales as shown in Fig. 5, two Be designs driven at 250 eV and at 300 eV, and a smooth-pulse 250-eV Be design. All except the PT scales shown in Fig. 5 use 1.1–1.5 MJ, at powers ranging from 365–500 TW. They give yields in the integrated simulations that are between 50–90% of clean 1-D yields and show unambiguous ignition.

Modeling asymmetry from imperfect power balance and pointing of the laser beams requires fully three-dimensional (3-D) asymmetry. This asymmetry has been estimated analytically using laser-spot brightness and positions determined from the 2-D LASNEX simulations. Also, the asymmetry has been calculated in 3-D with a view-factor code.[24] We have used fully integrated

calculations (described earlier) to confirm the modeling and for some sensitivity studies. The actual asymmetry on the capsule is 3-D, and its effect on the implosion must be estimated with 2-D simulations of the implosion driven with an asymmetric radiation source.

We have imposed a wide variety of asymmetries on 2-D capsule implosions to ensure that the specified asymmetry levels are acceptable. Asymmetry can affect ignition in a variety of ways: the obvious kinematic effects of differing velocities; initiation of RT instability growth, especially evident during deceleration; mass flow toward less driven regions, seeding RT instability; irregular hot-spot compression, sometimes forming jets that protrude from the core and disrupt the imploded configuration; and delayed ignition, resulting in more RT growth. The maximum tolerable asymmetry depends on its temporal and spatial specifics. In summary, the capsule can tolerate less than about 1% time-averaged asymmetry, 5–10% time-dependent swings in asymmetry that last for ~2 ns, and larger swings if they last much less than 2 ns.

We do not find much variation in sensitivity to asymmetry among the various targets we have designed. Smaller capsules are slightly more sensitive to asymmetries that couple to deceleration RT growth. The difference is not large, and symmetry sensitivity is not an issue that is important in deciding the overall trade-offs of laser size and power. Varying the hohlraum size, with a given capsule, is the symmetry issue likely to be more important in the trade-offs.

The 3-D view factor calculations indicate that with nominal pointing errors—each beam is to point within 50 μm of its nominal position, rms deviation—the resulting additional asymmetry on the capsule will be significantly <1%. This pointing specification also ensures more than adequate clearance of the LEH. This requirement is similar to that met by the Nova laser (30 μm rms,[25] which is 10 μrad, while 50 μm rms on NIF is 7 μrad because of the longer focal length).

The 3-D view factor calculations also indicate that 10% rms power imbalance results in <1% asymmetry on the capsule, provided the deviations are uncorrelated among the 192 beams. The tolerable power imbalance can be much larger than this, depending on its temporal dependence. If there are correlations between the beams' powers, a much tighter power balance requirement is necessary. Groups of eight beams, with each group entering the same area of the hohlraum, must be balanced within about 3%. Generally the requirements are consistent with purely independent statistical deviations of the 192 beams; any correlations significantly beyond this may increase the asymmetry unacceptably.

These requirements on the laser are well within current Nova performance parameters of 3% rms energy imbalance, and 5–10% power imbalance over time scales that are generally less than half the pulse length.[26] This does not mean that symmetry in Nova hohlraums is as good as in NIF hohlraums; the looser requirements for NIF are a result of the larger number of beams.

Asymmetries might also arise from laser–plasma interaction processes or other phenomena, such as RT instability at the Au / He interface, which are currently predicted not to be significant but for which uncertainty remains. Light can be scattered or it can be absorbed more or less efficiently at different positions in the hohlraum. The effect in all cases is equivalent to a power balance change, a movement of the x-ray emission spots, or perhaps a spreading of the laser deposition spots (for small-angle side-scattering). Difficulties could arise only if these effects are so large that the irreproducible part of them is larger than the limits described here. If any of these processes occurs but is reproducible and not too large, the effect can be compensated for by changing the hohlraum design parameters. Estimates based on Nova experiments and appropriate theory and modeling indicate that these processes can be kept within acceptable limits. If not, our ultimate recourse will be to increase the hohlraum size, reduce the laser intensity, and correspondingly reduce the hohlraum drive temperature.

Laser–Plasma Instabilities

The most important laser–plasma scattering processes are SBS, stimulated Raman scattering (SRS), and filamentation. In SBS and SRS, the incident laser beam scatters from electron waves and ion waves, respectively, in the forward, side, or backscatter direction. Backscatter is calculated and observed to be the most unstable process, although sidescatter must be examined for its possible effect on capsule symmetry. SRS forward scatter is a very weak process; forward SBS is being evaluated for possible symmetry effects because of the exchange of energy between overlapping beams.[27] Filamentation or whole-beam self focusing results from the refraction of the laser light into low-density regions, which are themselves produced by the pressure gradients from nonuniform laser heating or by ponderomotive forces. All of these processes are sensitive to the n_e and temperature, and laser intensity and wavelength.[28] In addition, SBS is sensitive to the electron-ion temperature ratio, velocity gradient, and the fraction of light and heavy ions in multiple species plasma.[29] Also, we have shown with 3-D filamentation simulations[30] that filamentation is sensitive to the speckle length (the axial length of a diffraction-limited hot spot near the focal plane of the laser beam). The speckle length increases with the square of the *f*-number of the focusing system.

The laser must propagate through 3–5 mm of hot (T_e ~ 3–5 keV at peak power), low-density ($n_e \leq 1 \times 10^{21}$ cm^{-3}), low-Z (mixture of He and H) plasma. The density is about 0.05 critical over most of the beam path. For the inner ring of beams, the density reaches as high as 15% of critical for the last millimeter

of pathlength. However, this far into the hohlraum the individual laser beam intensity has decreased substantially from its peak of 2×10^{15} W / cm^2.

These scattering processes affect the target performance in several ways. Of course, energy scattered back out of the hohlraum is unavailable for x-ray conversion. The total energy lost comes out of the ~50% energy margin shown in Fig. 2. The irreproducible part of this becomes a pulse-shape uncertainty, and any resultant geometrical nonuniformity can affect the symmetry of the irradiation on the capsule. These effects will be tolerable if the scattering is less than about 10%. We do not expect hot electrons produced by SRS to have any effect on target performance.

We estimate that the scattering processes will be acceptable under these predicted plasma conditions. Experimentally verifying these estimates is an action part of the Nova program, described in "Laser–Plasma Interactions in NIF-Scale Plasmas (HLP5 and HLP6)" on pg. 305 of this *Quarterly*.

Modeling of Hydrodynamic Instabilities

The shell is subject to RT instability on the outside during its acceleration and on the inside during deceleration. There is also Richtmyer–Meshkov (RM) instability at all interfaces. (These instabilities are reviewed in Ref. 31.) Short-wavelength RT growth in these capsules is stabilized by ablation of material through the unstable interface and by the finite scale length on the ablation front. Experimental[32] and calculational[33] aspects of this stabilization are well documented. During deceleration, the growth of short wavelengths is also reduced from classical RT since the unstable interface is between two DT regions, the hot spot and the main fuel, and again there is ablation (driven by electron conduction in this case) and a finite gradient scale length. Also, perturbations that grow on the outside must couple through the shell to affect the ignition, and short wavelength modes couple less effectively. These effects all reduce the impact of the short wavelengths, so the system is only weakly nonlinear. The targets have been designed so that this is the case.

We have based our modeling on linear analysis that is as accurate as possible, with an extension into the weakly nonlinear regime, as necessary. The linear analysis is based on a decomposition of the surface perturbations into spherical harmonics, which are eigenmodes of the linear evolution. We determine the single-mode growth spectrum by running multiple 2-D simulations, each of one single mode in the linear regime throughout the simulation. This provides the most accurate calculation of all known effects, including stabilization, RM growth, and convergence effects. This set of calculations provides a spectrum of growth factors, which we combine with an assumed initial surface spectrum to determine the ignition-time perturbation. Using a nonlinear saturation model from Ref. 34, we determine whether the perturbations are nonlinear and estimate the nonlinear saturation. This results in a curve of ignition-time perturbation amplitude as a function of initial perturbation amplitude.

To test the weakly nonlinear analysis, we also run full simulations of multimode perturbations with realistic initial amplitudes. Currently simulations must be 2-D, and the number of modes that can be included is limited. We have run a variety of multimode simulations on several capsules, at solid angles ranging from relatively small conic sections to half-spheres. Results are consistent with the modeling described earlier, although further substantiation is an area of current work. Recent development of 3-D codes will allow testing of possible differences between 2- and 3-D evolution.[35]

We must also estimate how the perturbations around the hot spot at ignition time will affect the ignition. The unstable interface is between relatively cold, dense DT and the hot, lower-density DT. Material mixing of different elements is not occurring, and there is only thermal mixing. The actual perturbations are 3-D, and multimode, and the weakly nonlinear perturbation growth analysis indicates that the spectrum is strongly dominated by mode numbers around l = 10–15°. The 3-D character cannot be fully represented in any existing code; available 3-D codes do not include all of the relevant physical processes. There is experimental[32] and calculational[35] evidence that the multimode 3-D perturbation is probably an array of spikes penetrating in toward the hot-spot center, surrounding approximately hexagonal bubbles. In 2-D, we modeled this array of spikes and bubbles five ways: (1) We simulated a single bubble of appropriate solid angle surrounded by a curtain of material falling along a reflecting boundary condition. The circular cone represents approximately a multifaceted 3-D cone of similar size and gross shape. (2) We ran perturbations with the opposite sign: a spike on axis surrounded by a circular bubble. (3) We simulated perturbations on the waist that represent long circular ridges and curtains. (4) We continued through burn time the multimode 2-D simulations mentioned earlier. (5) We did 1-D modeling in which the thermal mixing caused by the perturbation growth is represented as an enhanced thermal conductivity in the perturbed region.

All of these approaches give similar results, regarding how large a spike can be tolerated before ignition is quenched. Combined with the modeling described earlier, this corresponds to a maximum tolerable initial ablator surface roughness of about 50 nm rms. This compares with 30 nm rms on current Nova capsules.

We have also considered the bubble penetration from the outside of the shell at peak velocity. We find that the surface finish requirements for shell integrity during acceleration and for ignition are similar. This

equivalence depends weakly on the shape assumed for the spectrum of initial perturbations.

Because we have modeled the perturbation growth and its effects with a variety of different approaches, and get generally consistent results, we are fairly confident that our modeling is accurate. The modeling relies on 2-D code simulations of linear-regime perturbation growth, so it is very important that these be tested thoroughly. The dominant uncertainties are the dependence on the spectrum of the drive x rays, and on zoning, resulting in a net uncertainty in the outer surface finish specification that we believe to be about a factor of two. Finally, of course, it is very important to test the modeling experimentally. A major fraction of the Nova program is oriented toward verifying this modeling, with a variety of experiments measuring perturbation growth and its effects in planar[32] and spherical[5,10,36] geometry. Results from these experiments have been consistent with the modeling.

The modeling described so far pertains to surface perturbations that are initially on the outside of the ablator. Of course, there will be perturbations on the other interfaces, as well as material inhomogeneity and other fabrication defects. Any of these can be modeled in a conceptually identical way, using LASNEX simulations that assume the existence of the perturbation of interest. We have determined that the capsule tolerates perturbations initially on the other interfaces, which are much larger than tolerable perturbations initially on the outside. Perturbations on the DT/CH interface are unlikely to be large enough to matter. Ignition does not occur if perturbations on the DT gas/solid interface are greater than about 3.0 μm for the PT, and more than about 8 μm for Be capsules, which are the same size as the PT and are driven at 300 eV. Current estimates[37] of the smoothness of β layer surfaces are ~1 μm. Solid DT in a low-density foam is somewhat smoother.

In summary, the PT has a factor of about two margin in surface finish beyond surface finishes on the best current Nova capsules. The requirement on the DT gas/solid interface also gives about a factor of 2 margin compared with roughness measured on recent DT ice surfaces.

Robustness Studies

We performed extensive studies of the robustness of the PT target following the initial design work, which we categorize into two studies discussed below.

Robustness of Yield in Integrated Simulations

Choosing a particular configuration as nominal, we varied the laser powers and pointing in detailed integrated calculations (described earlier). Figure 4 is an example of such a variation (although the calculations shown there used a laser pulse slightly different from what we chose as nominal for the full set of variations). Table 1 shows the sensitivities we found, and compares them with estimates of the reliability with which we can determine and maintain these parameters. This study produced three valuable results. (1) We verified that the target can tolerate plausible variations in the input parameters (shown in Table 1). This allays concern that the performance of the target is a finely tuned optimum that would be impossible to achieve experimentally. (2) We identified ways in which the configuration we chose as nominal was not in fact optimal (most importantly, we found significant room for improvement in the pointing we were using for the inner cone). We are currently doing a second iteration, with improved pointing and better optimization of the other parameters, which should show a margin of performance even larger than that shown in Table 1. Some results of the study with the new optimization are shown in Table 1. (3) This study provides a context for designing the experimental campaign to achieve ignition. Table 1 (and subsequent revisions) shows which parameters must be measured and maintained and to what accuracy.

We are also doing integrated simulations varying several parameters at once. We have varied both the inner and outer cone laser powers separately (in addition to the variations shown in Table 1), and see sensitivity similar

TABLE 1. Sensitivity analysis of the PT using integrated calculations of the entire hohlraum/capsule target.

Laser parameter*	Determined sensitivities	Preliminary estimate
Power during foot	30%	<5%
Peak power	35%	<5%
Second-rise timing	500 ps	<100 ps
Third-rise timing	500 ps	<100 ps
Duration of peak power	800 ps	<100 ps
Inner beam power during foot (total power fixed)	25%	<5%
Inner beam power during peak (total power fixed)	35%	<5%
Inner beam power during peak (outer cone power fixed)	25%	<5%
Pointing of inner beams	85 μm (200 μm)†	<20 μm
Pointing of outer beams	100 μm (350 μm)†	<20 μm

*For each indicated parameter describing the laser input power, we tabulated the full-width at half maximum of the yield as that parameter was varied. We also tabluated estimates of the precision with which the parameters can be determined and maintained in an experimental campaign working toward ignition. In all cases, the indicated precision is dominated by estimates of experimental precision, and the corresponding specification on the laser itself is significantly smaller.

†These values are for a new optimization with the P_6 asymmetry reduced.

to that shown in Table 1. Ultimately we will explore the entire parameter space of possible variations, although we will use the new nominal design mentioned above instead of continuing to center the variations on our first preliminary optimization.

Sensitivity to Combinations of Asymmetry, Pulse-Shaping Errors, and Hydrodynamic Instabilities

To create a complete model for what could affect the implosion adversely, we utilized a series of capsule-only simulations. We started by simulating the capsule with the asymmetry determined from the nominal integrated calculation, then added perturbed surfaces, and finally added asymmetric drive sources. The asymmetry can be made to match that in the integrated calculations by extracting from the integrated simulation the asymmetry in ablation pressure in the imploding capsule. (The asymmetry can be characterized with Legendre polynomial moments, with P_2 through P_6 contributing.) Then a matching radiation drive asymmetry, in a simulation of the capsule alone, produces an identically out-of-round implosion. This technique matches the asymmetry both for a nominal design and for the off-nominal integrated calculations represented in Table 1. (We chose as nominal the same integrated calculation used as the central point for the variations presented in Table 1). We performed three variations given the "baseline" nominal asymmetric implosion.

1. Asymmetry alone. We found that the "nominal" asymmetry has about 50% margin in the P_6 moment and >100% margin in the P_2 and P_4 moments. This suggests that the overall robustness can be improved by reoptimizing to minimize P_6. This is part of the reoptimization mentioned above, increasing further the margin of the PT.
2. Nominal asymmetry plus short-wavelength surface roughness. We performed implosions with the nominal asymmetry and perturbations on both the inner and outer capsule surfaces. The spectral features of the perturbations were based on characterization of β layered DT for the ice roughness and of Nova CH capsule surface roughness for the outside. The capsule ignites and burns well with nominal asymmetry and nominal surface roughnesses of 30 nm on the CH and 1.0 μm on the DT.
3. Off-nominal asymmetry and drive, plus short-wavelength surface roughness. In addition to the nominal asymmetry, we included further random asymmetry—up to 4.5% rms P_2 and 1.5% rms P_4. The additional asymmetry was a random function of time, with zero mean and about 2 ns typical period of variation. We also included variations in the drive profile (the net flux onto the capsule, P_0) of ±5%. The combination of asymmetry, drive profile errors, and surface roughness represents the most complete possible model of the implosion. We found that the additional asymmetry and profile variations had little effect on the yield; for example, with 30 nm outer roughness and 1.0 μm inner roughness, we obtain 11.5 MJ of yield with the nominal asymmetry plus the variations of 4.5% rms P_2, 1.5% rms P_4, and ±5% P_0.

These robustness results are extremely encouraging assurance of the nominal design's performance.

Summary

Given the experimental substantiation from the Nova program, we have good reason to expect ignition with a 1.8-MJ, 500-TW laser. Such a laser will provide an adequate safety margin, above the ignition threshold indicated by modeling supported by Nova experiments. This margin is sufficient to cover estimated uncertainties.

We can compensate for the remaining uncertainties by adjusting the target design if necessary after additional Nova experiments, or after the NIF experiments begin. Some possible changes in the target design or performance will be energetically significant. These include:

- A factor of two in hydrodynamic instability growth (equivalent to a factor of two in surface finish, or a factor of two in the acceptable size of the bang-time perturbations) shifts the ignition cliff from 0.8 MJ to about 1.0 MJ. Improvements in surface finish could probably recover the original margin.
- The combined uncertainties in x-ray conversion and hohlraum wall loss are less than about 20% in energy.
- SBS and SRS should be less than about 10%, based on the experiments described in "Laser–Plasma Interactions in NIF-Scale Plasmas (HLP5 and HLP6)" on pg. 305 of this *Quarterly*.
- Achieving the correct power balance between the inner and outer cones of beams may require reducing the power in one or the other, so that it cannot run at its full power. This may result in a net energy loss of 10–15%.
- An error in hohlraum optimization that requires increasing the LEH radius 50% would require an increase in laser energy of 15% to regain the same hohlraum temperature.
- Similarly, increasing the hohlraum area by 35% increases the required laser energy by 15%.

Several other uncertainties are energetically insignificant. For example, the EOS and opacity of the CH ablator are sufficiently uncertain that we expect to adjust the details of the pulse shape phenomenologically, but this will not significantly affect the performance

requirements from the laser or the target performance. These errors, in combined effect, are consistent with the factor of two margin provided by a 1.8-MJ, 500-TW laser.

There are some issues that we are addressing to substantiate this conclusion further and to progress with plans for the facility. We need to make a final decision regarding the optimal cone-to-cone energy ratio, and beam angles, which will be built into the target chamber and will be difficult to change once detailed facility design is in progress. To maximize our understanding of the options available to us, we are continuing to pursue other designs—e.g., hohlraums with shields between the capsule and the LEH. Finally, we also continue to pursue more detailed modeling of the PT. These results, along with the ongoing experimental program on Nova, will either lead to increasing confidence in the performance of the PT or will indicate what changes need to be made in the design.

Notes and References

1. J. H. Nuckolls, L. Wood, A. Thiessen, and G. B. Zimmerman, *Nature* 239, 129 (1972).
2. J. D. Lindl, R. L. McCrory, E. M. Campbell, *Physics Today* (Sept. 1992).
3. J. T. Hunt, K. R. Manes, J. R. Murray, P. A. Renard, et al., "Laser Design Basis for the National Ignition Facility," Lawrence Livermore National Laboratory, Livermore, CA, UCRL-JC-117399 (1994).
4. S. W. Haan et al., *Phys. Plasmas* 2(6) (1995).
5. C. Verdon, Laboratory for Laser Energetics, Rochester, NY, private communication (1994).
6. J. D. Lindl, "Development of the Indirect-Drive Approach to Inertial Confinement Fusion and the Target Physics Basis for Ignition and Gain," UCRL-JC-119015218 (1995); submitted to *Phys. Plasmas* (1995).
7. A. J. Martin, R. J. Simms, and R. B. Jacobs, *J. Vac. Sci. Technol.* A 6(3), 1885 (1988).
8. S. N. Dixit, J. K. Lawson, K. R. Manes, H. T. Powell, and K. A. Nugent, *Opt. Lett.* 9, 417–419 (1994).
9. R. L. Kauffman, L. J. Suter, C. B. Darrow, J. D. Kilkenny, et al., *Phys. Rev. Lett.* 73, 2320–2323 (1994).
10. C. J. Keane, R. C. Cook, T. R. Dittrich, B. A. Hammel, et al., "Diagnosis of Pusher–Fuel Mix in Spherical Implosions Using X-Ray Spectroscopy," Lawrence Livermore National Laboratory, Livermore, CA, UCRL-JC-116787 (1994); submitted to *Rev. Sci. Inst.* (1995).
11. G. B. Zimmerman and W. L. Kruer, *Comm. Plasmas Phys. Cont. Thermonuclear Fusion* 2, 51 (1975).
12. D. S. Kershaw, "Flux Limiting in Nature's Own Way," Lawrence Livermore National Laboratory, Livermore, CA, UCRL-78378 (1976).
13. R. M. More, K. H. Warren, D. A. Young, and G. B. Zimmerman, *Phys. Fluids* 31(10), 3059 (1988).
14. W. A. Lokke and W. H. Grasberger, "XSNQ-U: A NonLTE Emission and Absorption Coefficient Subroutine," Lawrence Livermore National Laboratory, Livermore, CA, UCRL-52276 (1977).
15. E. G. Corman, W. B. Loewe, G. E. Cooper, and A. M. Winslow, *Nucl. Fusion* 15, 377 (1975).
16. S. P. Hatchett, Lawrence Livermore National Laboratory, Livermore, CA, private communication (1993).
17. G. B. Zimmerman, "Recent Developments in Monte-Carlo Techniques," Lawrence Livermore National Laboratory, Livermore, CA, UCRL-105616 (1990).
18. A. K. Burnham, J. Z. Grens, E. M. Lilley, *J. Vac. Sci. Technol.* A 5(6), 3417 (1987).
19. P. C. Souers, *Hydrogen Properties for Fusion Energy* (University of California Press, Berkeley, CA, 1986).
20. R. A. Sacks and D. H. Darling, *Nuc. Fus.* 27, 447 (1987).
21. P. A. Amendt, Lawrence Livermore National Laboratory, Livermore, CA, private communication regarding symmetry tuning and increased x-ray drive in modified Nova hohlraums, to be published in *Phys. Rev. Lett.* (1995).
22. A. Hauer, et al., *Phys. Plasmas* 2(6) (1995).
23. A. Bar Shalom, J. Oreg, W. H. Goldstein, D. Shvarts, and A. Zigler, *Phys. Rev.* A 40, 3183 (1989).
24. R. C. Kirkpatrick and C. A. Wingate, Los Alamos National Laboratory, Los Alamos, NM, private communication (1980); R. C. Kirkpatrick, J. E. Tabor, E. L. Lindman, A. J. Cooper, "Indirect Solar Loading of Waste Heat Radiators," *Proc. Space 88*, S. W. Johnson and J. P. Wetzel, Eds. (the American Society of Civil Engineers, 1988) p. 964; D. S. Bailey (1981), D. H. Munro and G. B. Zimmerman (1993), Lawrence Livermore National Laboratory, Livermore, CA, private communication.
25. J. E. Murray, M. C. Rushford, C. S. Vann, R. L. Saunders, and J. A. Caird, *ICF Quarterly Report* 4(1), 18, Lawrence Livermore National Laboratory, Livermore, CA, UCRL-LR-105821-94-1 (1993).
26. J. A. Caird, R. B. Ehrlich, O. L. Landen, C. W. Laumann, et al., *ICF Quarterly Report* 4(1), 10, Lawrence Livermore National Laboratory, Livermore, CA, UCRL-LR-105821-94-1 (1993).
27. K. Marsh, C. Joshi, and C. J. McKinstrie, *BAPS* 39, 1585, Minneapolis, MN, November 7–11, 1994.
28. W. L. Kruer, *The Physics of Laser Plasma Interactions* (Addison–Wesley, NY, 1998).
29. E. A. Williams, R. L. Berger, R. P. Drake, A. M. Rubenchik, et al., *Physics of Plasmas* 2, 129 (1995); S. C. Wilks, W. L. Kruer, J. Denavit, K. Estabrook, et al., "Nonlinear Theory and Simulations of Stimulated Brillouin Backscatter in Two and Three Species Plasmas," Lawrence Livermore National Laboratory, Livermore, CA, UCRL-JC-117313 (1995); accepted for publication in *Phys. Rev. Lett.*
30. R. L. Berger et al., *Phys Fluids B* 5, 2243 (1993).
31. S. W. Haan, "Hydrodynamic Instabilities on ICF Capsules," Lawrence Livermore National Laboratory, Livermore, CA, UCRL-JC-107592 (1991); to be published in *Lecture Series on Inertial Fusion*, Dept. of Astrophysical Sciences, Princeton University.

32. B. A. Remington, S. V. Weber, S. W. Haan, J. D. Kilkenny, et al., *Phys. Fluids B* 5, 2589 (1993).
33. S. V. Weber, B. A. Remington, S. W. Haan, B. G. Wilson, and J. K. Nash, *Phys. Plasmas* 1, 3652 (1994); H. Takabe, K. Mima, L. Montierth, and R. L. Morse, *Phys. Fluids* 28, 3676 (1985); M. Tabak, D. H. Munro, and J. D. Lindl, *Phys. Fluids B* 2, 5 (1990); J. H. Gardner, S. E. Bodner, and J. P. Dahlburg, *Phys. Fluids B* 3, 1070 (1991).
34. S. Haan, *Phys. Rev. A* 39, 5812 (1989).
35. J. P. Dahlburg et al., *Phys. Plasmas* 2(6), (1995); M. Marinak, Lawrence Livermore National Laboratory, Livermore, CA, private communication (1994).
36. T. R. Dittrich, B. A. Hammel, C. J. Keane, R. McEachern, et al., *Phys. Rev. Lett.* 73, 2324–2327 (1994).
37. G. W. Collins, E. R. Mapoles, J. Hoffer, J. Simpson, et al., *ICF Quarterly Report* 3(2), 81, Lawrence Livermore National Laboratory, Livermore, CA, UCRL-LR-105821-93-2 (1993).